Soft-templated synthesis of hierarchical micro- and mesoporous Zn/Co bimetallic zeolitic imidazolate frameworks

Keisuke Shirasaki, [a] Yingji Zhao, *[a] Yusuke Asakura [a] and Yusuke Yamauchi *[a,b,c]

[a]Department of Materials Process Engineering, Graduate School of Engineering, Nagoya University, Nagoya, Japan.

[b] Australian Institute for Bioengineering and Nanotechnology (AIBN) and School of Chemical Engineering, The University of Queensland, Brisbane, Queensland, Australia

c.Department of Chemical and Biomolecular Engineering, Yonsei University, 50 Yonsei-ro, Seodaemun-gu, Seoul 03722, South Korea.

Chemicals

All chemicals were commercially available and used without further purification. Zinc nitrate hexahydrate (99%), cobalt nitrate hexahydrate (98%), Acetone (99%) were purchased from Fujifilm Wako Pure Chemical Co., Ltd. (JP). Ethanol (99.5%) was purchased from Kishida Chemical Co., Ltd. (JP). 2-MIM (99%) was obtained from Sigma-Aldrich Technologies. PS_{5000}-*b*-PEO_{2500} was purchased from Polymer Source, Inc. (Product ID : P40298-SEO).

Method

First, 9 mg of PS5000-b-PEO2500 was dissolved in 100 μL of THF. Then, 2 mL of an aqueous 2-MIM solution was added under stirring. After 10 minutes of stirring at room temperature, 2 mL of a 40 mM mixed aqueous solution of $Zn(NO_3)_2 \cdot 6H_2O$ and $Co(NO_3)_2 \cdot 6H_2O$ was rapidly injected into the mixture. The solution was stirred for 5 minutes and then left undisturbed for 4 hours. The resulting product was collected by centrifugation at 10,000g for 5 minutes, followed by washing four times with ethanol and acetone.

For washing, ethanol or acetone was added to the centrifuge tube containing the product, then ultrasonicated for 10 minutes. The solution was subsequently centrifuged at 10,000g for 5 minutes. This process was repeated four times: ethanol was used for the first and fourth washes, while acetone was used for the second and third. Finally, the product and dried overnight at 60°C to obtain Zn_XCo_Y-mZIF-Z, where X:Y represents the Zn:Co ratio in the mixed solution and Z indicates the concentration of the 2-MIM solution.

X-ray Diffraction (XRD)

XRD data was collected using a Rigaku SmartLab X-ray diffractometer at a scan rate of 5° min^{-1} with a Cu Kα radiation source operating at 40 kV and 30 mA.

Scanning Electron Microscopy (SEM)

SEM images were taken using a ZEISS GeminiSEM 560 scanning electron microscope at an acceleration voltage of 2 kV.

Nitrogen Adsorption-Desorption Isotherms

Nitrogen adsorption-desorption isotherms were measured using a MicrotracBEL Corp. BEL-mini instrument after degassing the sample for 10 h at 100 ºC. BJH poresize distribution was calculated from adsorption branch.

Transmission Electron Microscopy and Energy Dispersive X-ray Spectroscopy (TEM-EDS)

TEM-EDS was performed using a JEOL JEM-2100 Plus operating at 200 kV.

Dynamic Light Scattering (DLS)

DLS measurements were conducted using an Otsuka ELSZ-2000.

X-ray Photoelectron Spectroscopy (XPS)

XPS was carried out with ULVAC-PHI, INC. PHI Quantes.

Thermogravimetric Analysis (TGA)

TGA was conducted using a Rigaku TG-DTA 8122.

Ultraviolet Diffuse Reflectance Spectroscopy (UV-DRS)

UV-DRS measurements were performed using a JASCO V-770.

Fourier Transform Infrared Spectroscopy (FT-IR)

FT-IR spectra were recorded using a JASCO FT/IR 4X.

Inductively Coupled Plasma (ICP)

ICP results were obtained using a Seiko SII SPS7800 Plasma Spectrometer.

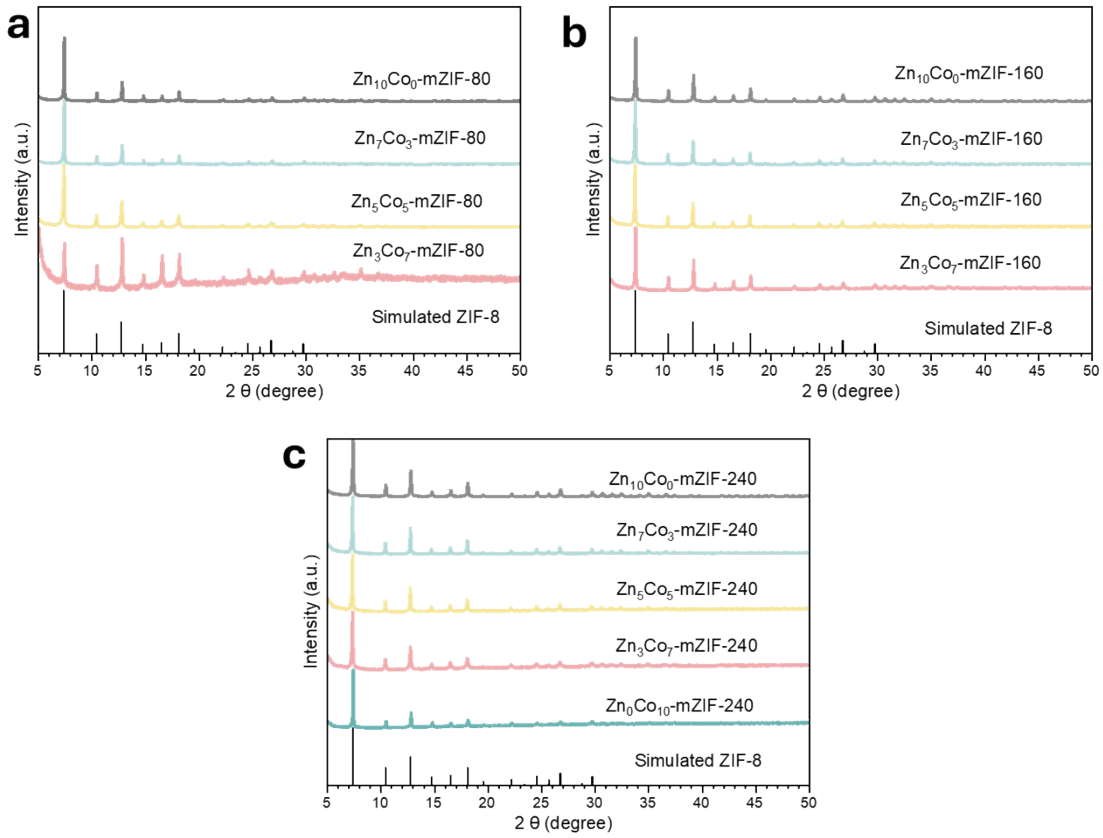

Fig. S1 XRD pattern of (a) Zn_XCo_Y-mZIF-80, (b) Zn_XCo_Y-mZIF-160 and (c) Zn_XCo_Y-mZIF-240.

Due to the extremely low yield of the solid product, it was difficult to obtain meaningful XRD data of Zn_0Co_{10}-mZIF-80 and Zn_0Co_{10}-mZIF-160.

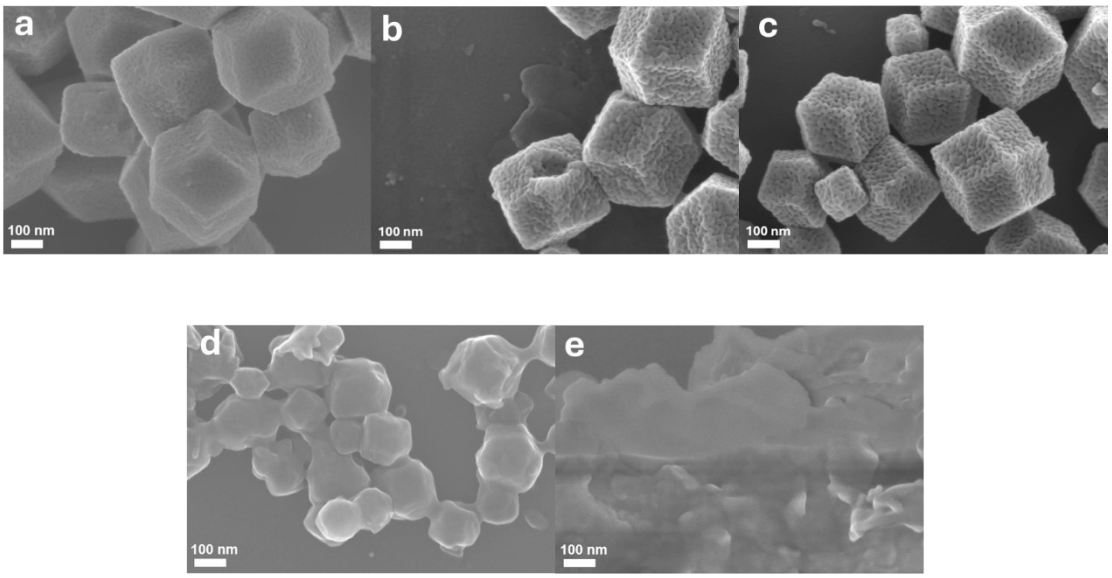

Fig. S2 SEM images of (a) $Zn_{10}Co_0$-mZIF-80, (b) Zn_7Co_3-mZIF-80, (c) Zn_5Co_5-mZIF-80, (d) Zn_3Co_7-mZIF-80 and (e) Zn_0Co_{10}-mZIF-80.

During the aqueous synthesis of ZIF-8, the coordination between metal ions and 2-MIm competes with hydrolysis by water molecules. Moreover, the formation of ZIF-67 generally requires a higher 2-MIm/metal ion ratio than ZIF-8. Given these factors, it is possible that cobalt hydroxide ($Co(OH)_2$) was formed instead at a lower Zn/Co ratio.

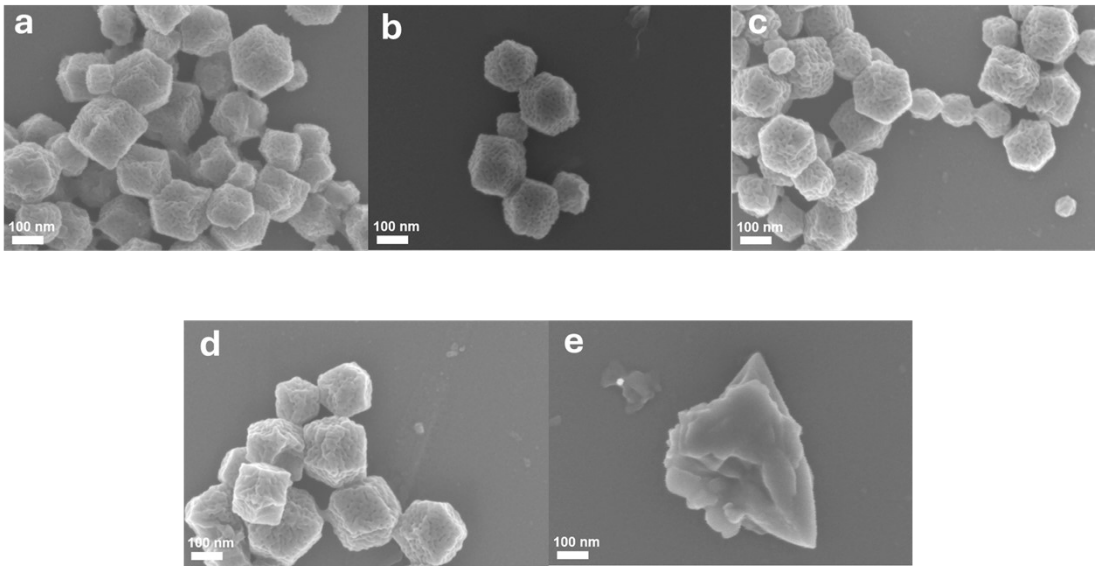

Fig. S3 SEM images of (a) $Zn_{10}Co_0$-mZIF-160, (b) Zn_7Co_3-mZIF-160, (c) Zn_5Co_5-mZIF-160, (d) Zn_3Co_7-mZIF-160 and (e) Zn_0Co_{10}-mZIF-160.

For the same reason as in Fig. S2d and S2e, $Co(OH)_2$ is considered to have formed under the synthesis conditions of Zn0Co10-mZIF-160.

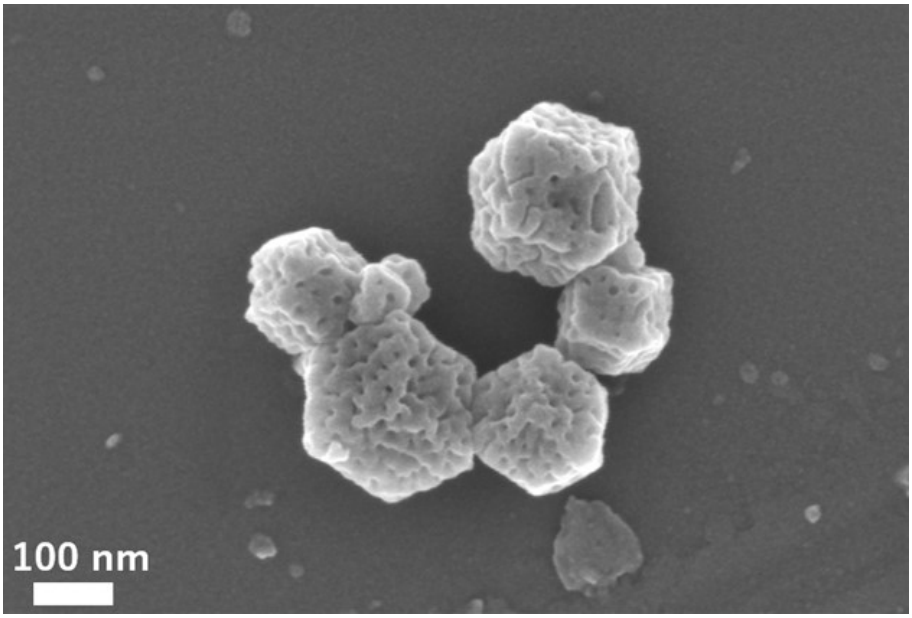

Fig. S4 SEM image of partially cracked Zn_5Co_5-mZIF-240.

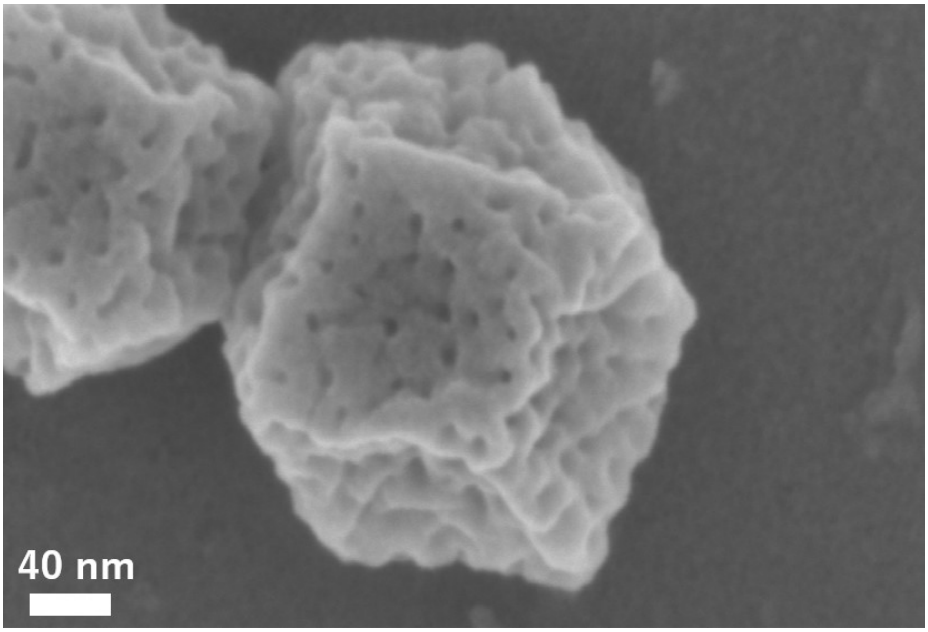

Fig. S5 Higher-magnification SEM image of Zn_5Co_5-mZIF-240.

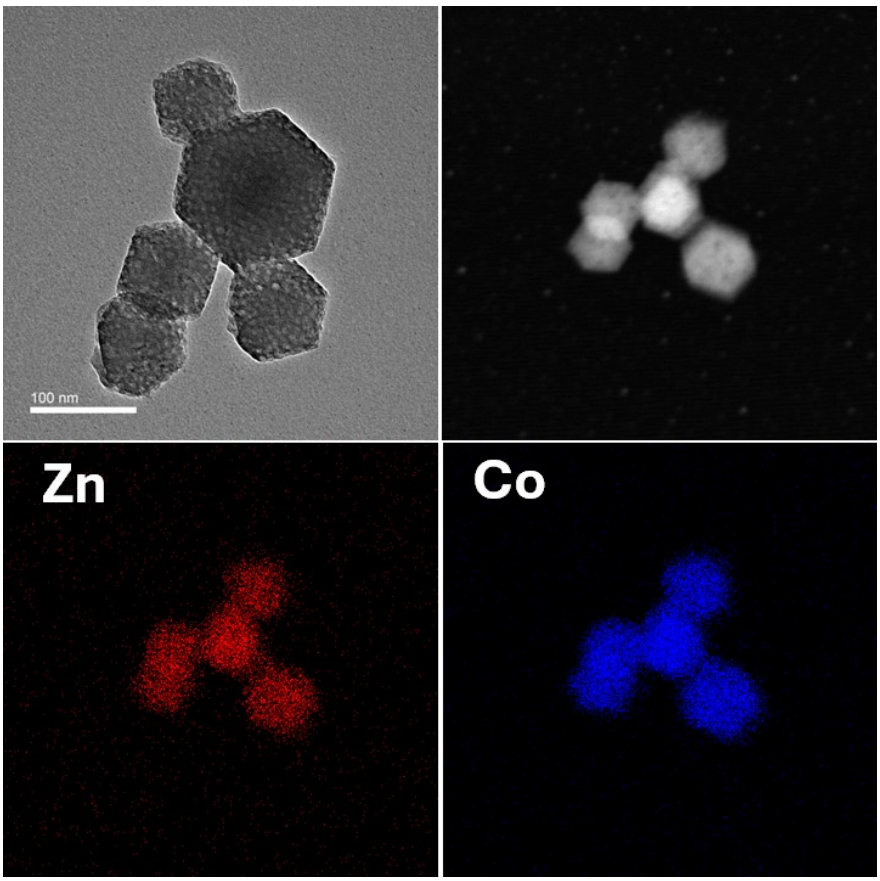

Fig. S6 TEM and EDS results of Zn_5Co_5-mZIF-240.

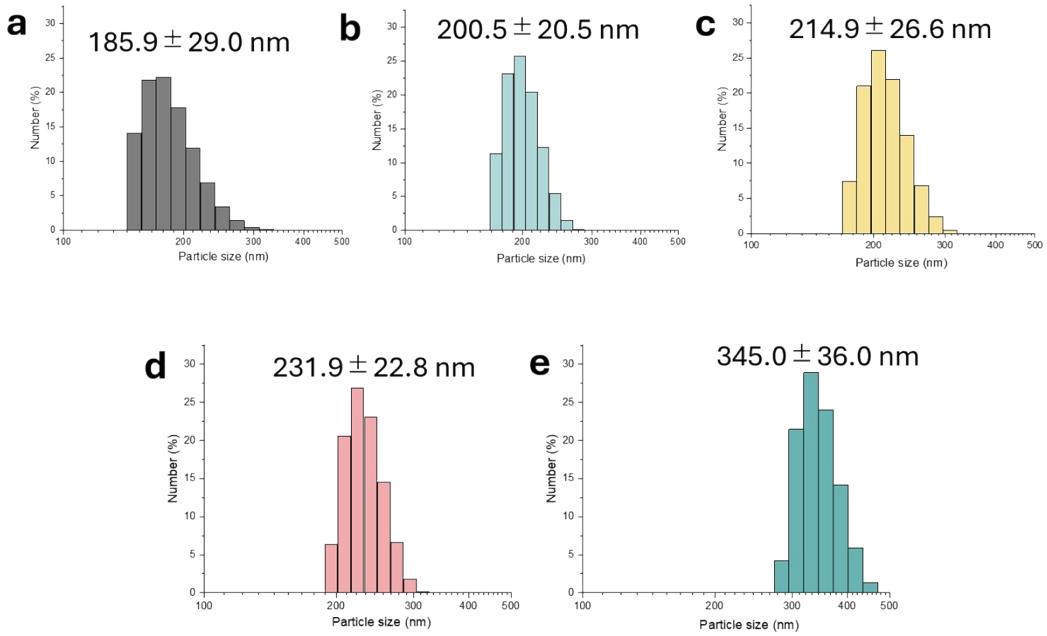

Fig. S7 DLS results of (a) $Zn_{10}Co_0$-mZIF-240, (b) Zn_7Co_3-mZIF-240, (c) Zn_5Co_5-mZIF-240, (d) Zn_3Co_7-mZIF-240 and (e) Zn_0Co_{10}-mZIF-240.

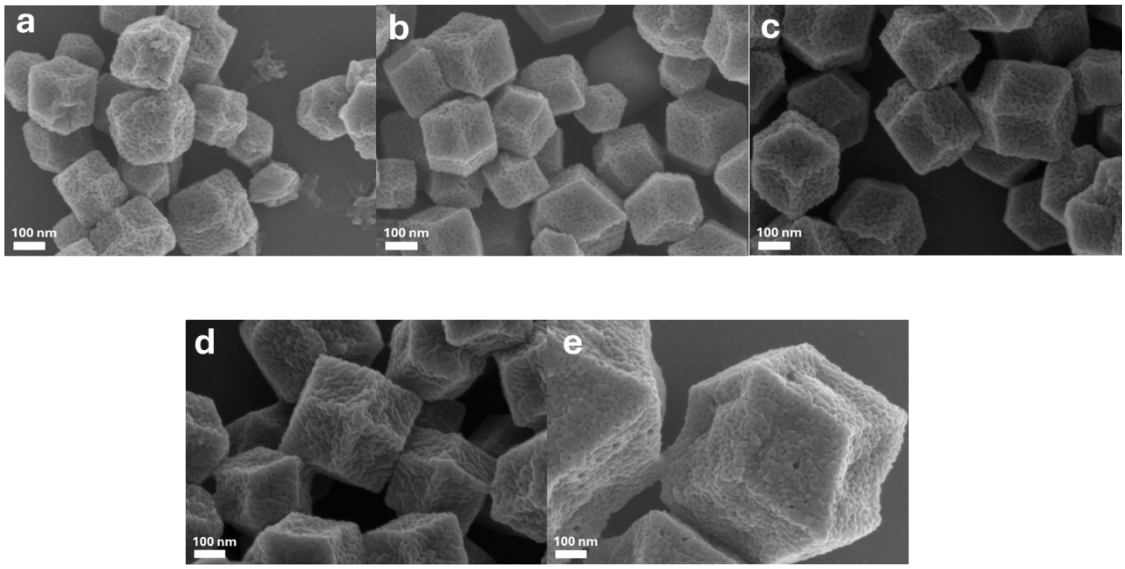

Fig. S8 SEM images of (a) $Zn_{10}Co_0$-mZIF-240, (b) Zn_7Co_3-mZIF-240, (c) Zn_5Co_5-mZIF-240, (d) Zn_3Co_7-mZIF-240 and (e) Zn_0Co_{10}-mZIF-240 synthesized at 0℃.

Table S1 BET surface area and pore volume of Zn_XCo_Y-mZIF-240

Sample	BET surface area[m^2/g]	Pore volume[cm^3/g]
$Zn_{10}Co_0$-mZIF-240	1354	1.05
Zn_7Co_3-mZIF-240	1407	1.34
Zn_5Co_5-mZIF-240	1359	0.94
Zn_3Co_7-mZIF-240	1262	0.72
Zn_0Co_{10}-mZIF-240	1140	0.57

For the BET analysis, we selected the pressure range where the (p/p_0) values were below 0.1, as the data in this range was visually clearly linear. Additionally, we confirmed that the C value was positive and within the range typically observed for adsorbents, which is usually in the order of several hundred.

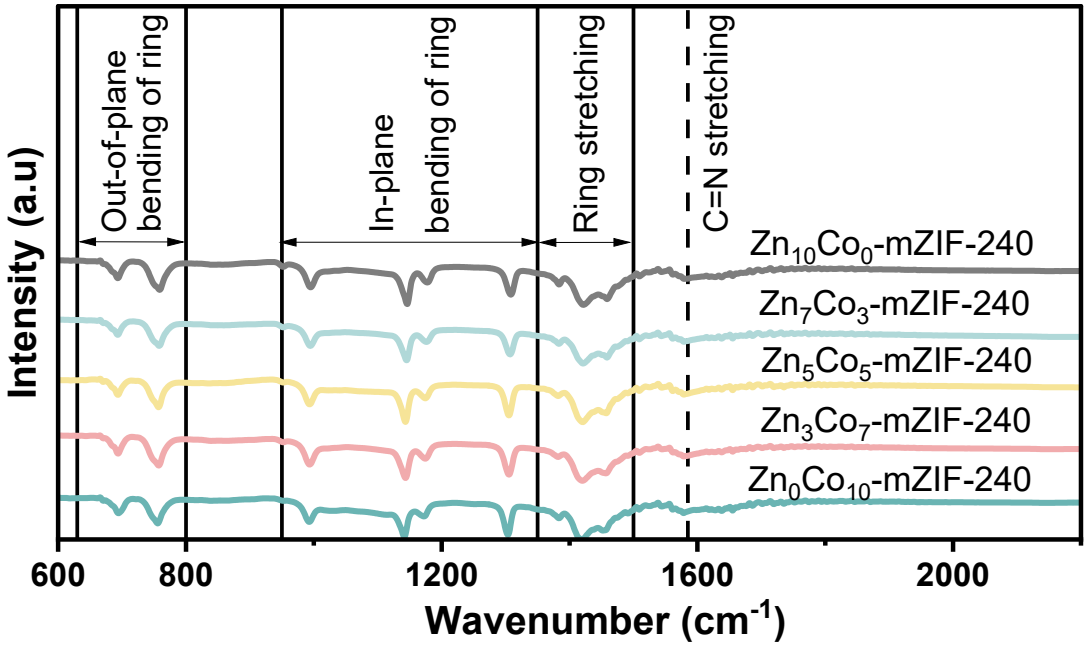

Fig. S9 FT-IR spectra of Zn_XCo_Y-mZIF-240.

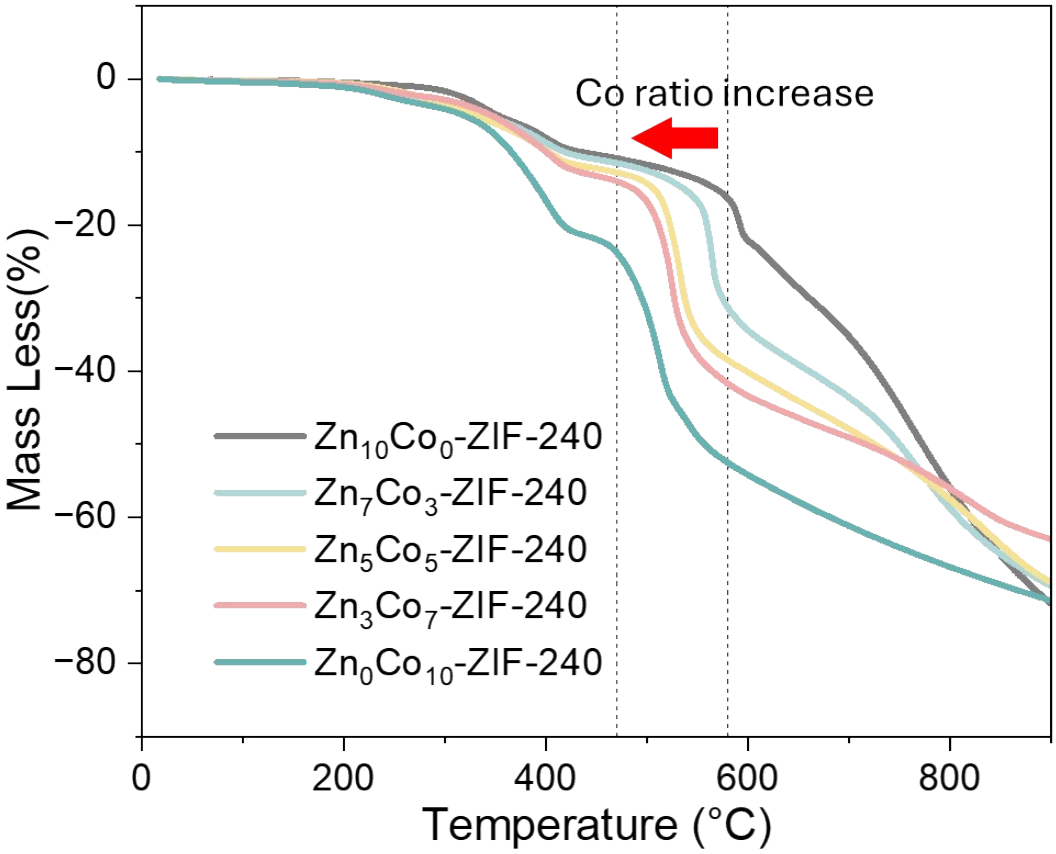

Fig. S10 TGA of Zn_XCo_Y-mZIF-240.

Table S2 Molar ratio of ZnCo-mZIF calculated from XPS measurements, along with the Zn:Co values obtained from both XPS and ICP analysis.

Sample	C1s	N1s	O1s	Zn2p3	Co2p	Zn : Co (XPS)	Zn : Co (ICP)
Zn_5Co_5-mZIF-80	65.3	23.4	3.4	7.8	0.1	98 : 2	n.a.
Zn_5Co_5-mZIF-160	66.3	23.1	3.3	5.6	1.7	77 : 23	80 : 20
$Zn_{10}Co_0$-mZIF-240	61.7	24.5	3.9	9.9	0.0	100 : 0	n.a.
Zn_7Co_3-mZIF-240	62.0	23.4	5.0	7.6	2.0	80 : 20	79 : 21
Zn_5Co_5-mZIF-240	63.8	25.0	3.2	4.8	3.2	60 : 40	59 : 41
Zn_3Co_7-mZIF-240	65.5	21.5	3.9	3.9	5.2	43 : 57	39 : 61
Zn_0Co_{10}-mZIF-240	64.1	18.9	7.9	0.0	9.1	0 : 100	n.a.

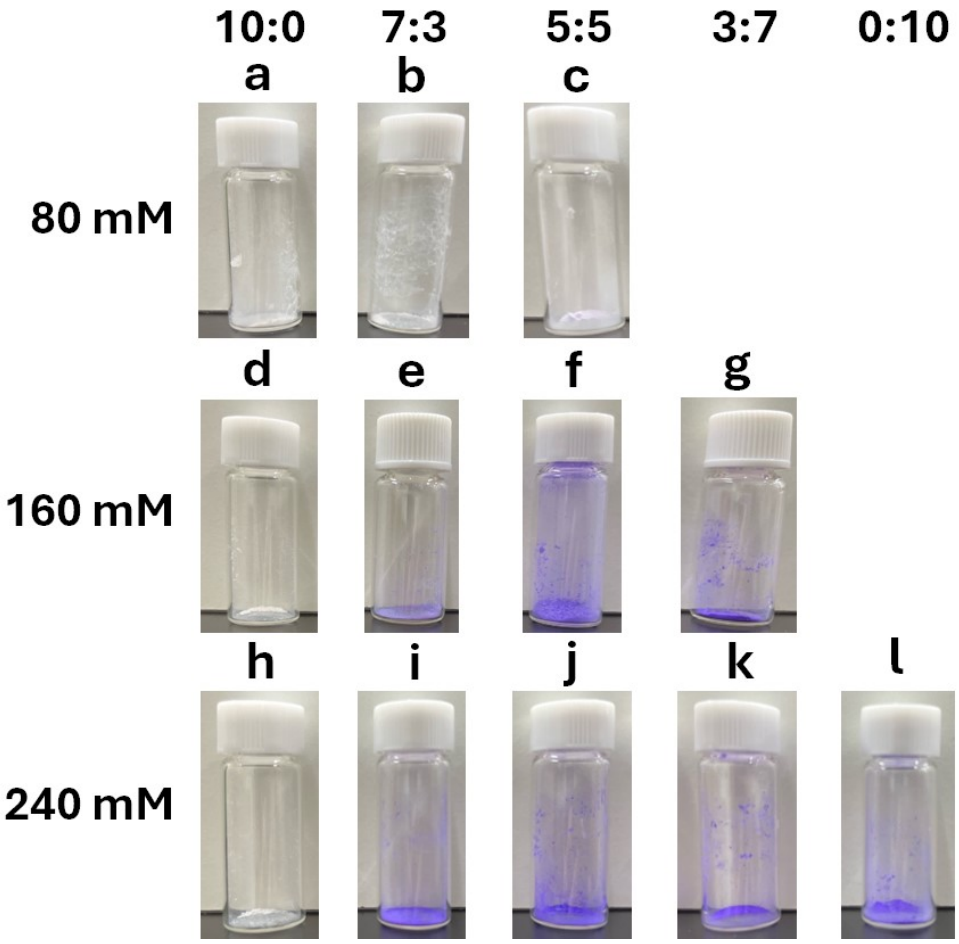

Fig. S11 Photographs of (a)-(c) Zn_XCo_Y-mZIF-80, (d)-(g) Zn_XCo_Y-mZIF-160 and (h)-(l) Zn_XCo_Y-mZIF-240.

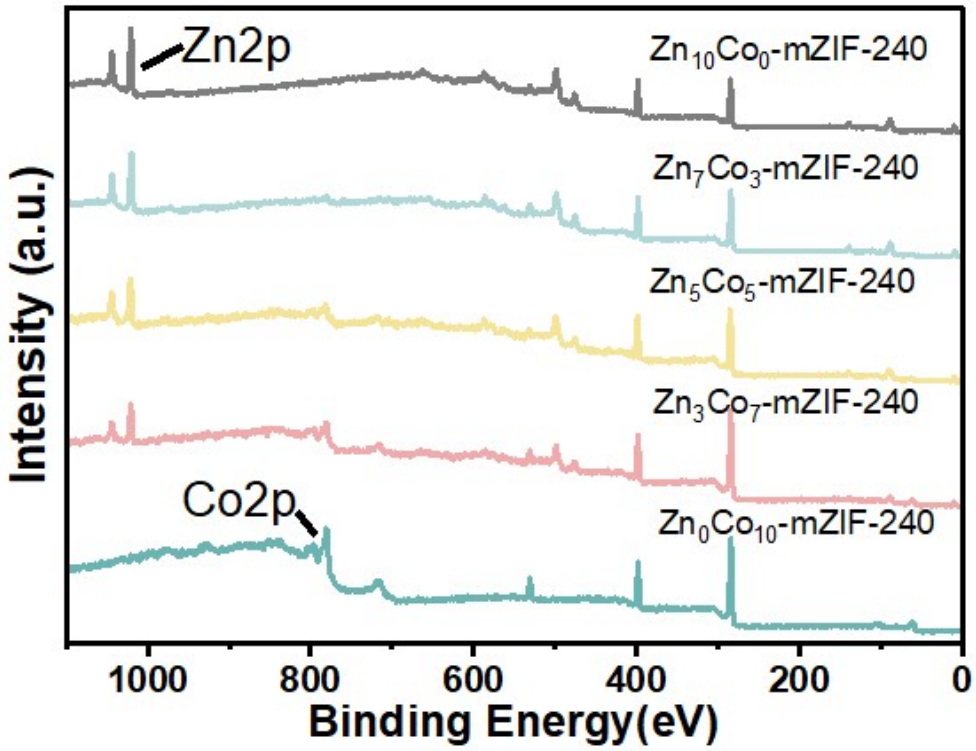

Fig. S12 Survey spectra of Zn_XCo_Y-mZIF-240.

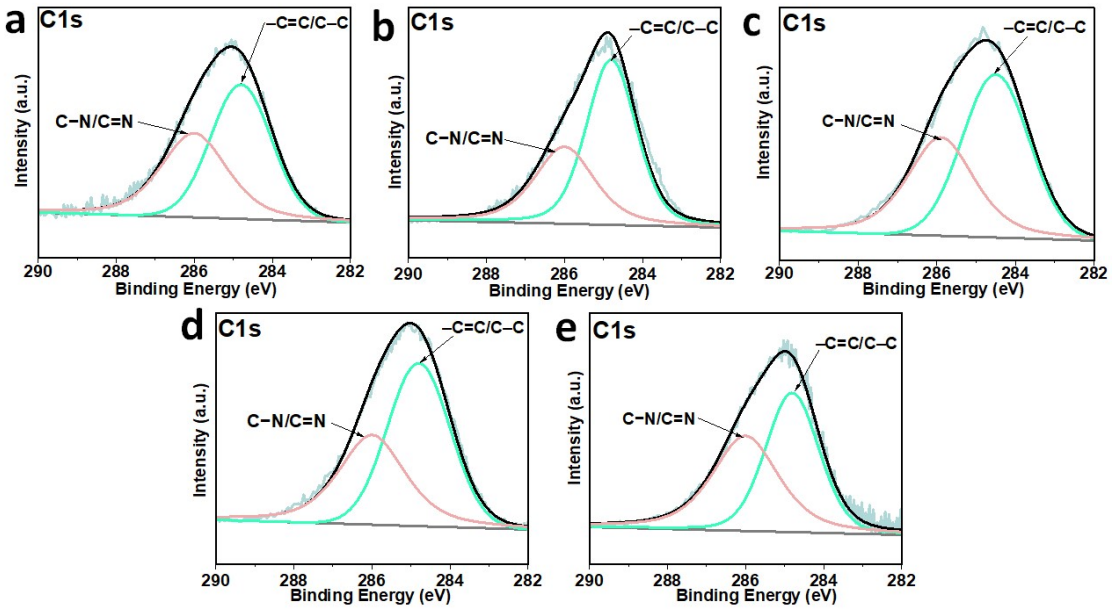

Fig. S13 C1s spectra of (a) $Zn_{10}Co_0$-mZIF-240, (b) Zn_7Co_3-mZIF-240, (c) Zn_5Co_5-mZIF-240, (d) Zn_3Co_7-mZIF-240 and (e) Zn_0Co_{10}-mZIF-240.

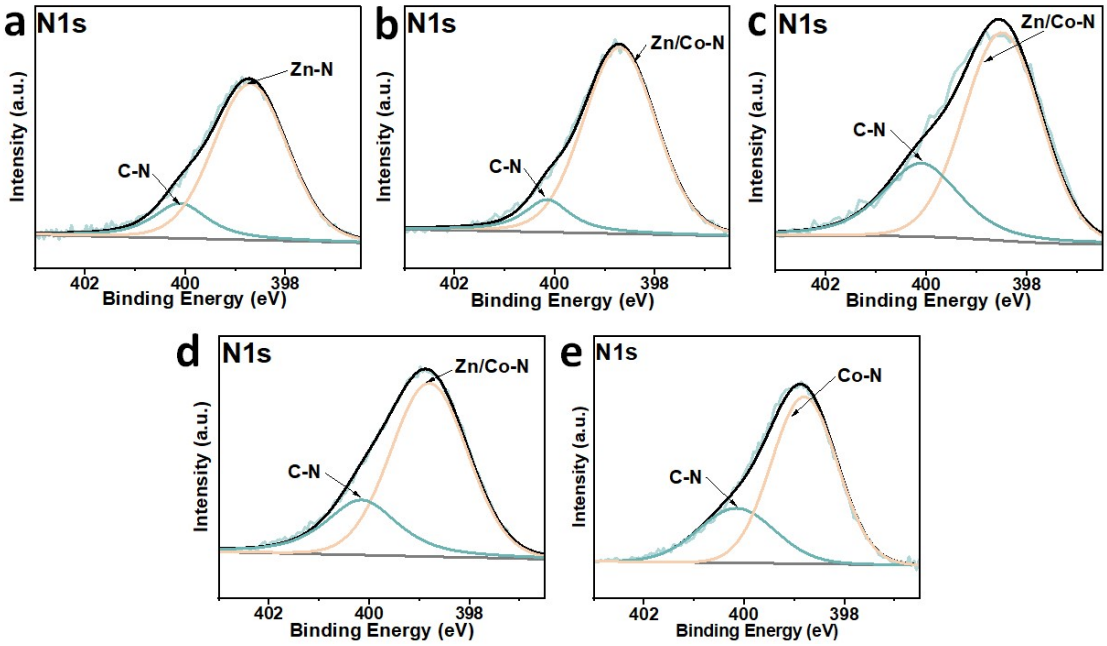

Fig. S14 N1s spectra of (a) $Zn_{10}Co_0$-mZIF-240, (b) Zn_7Co_3-mZIF-240, (c) Zn_5Co_5-mZIF-240, (d) Zn_3Co_7-mZIF-240 and (e) Zn_0Co_{10}-mZIF-240.

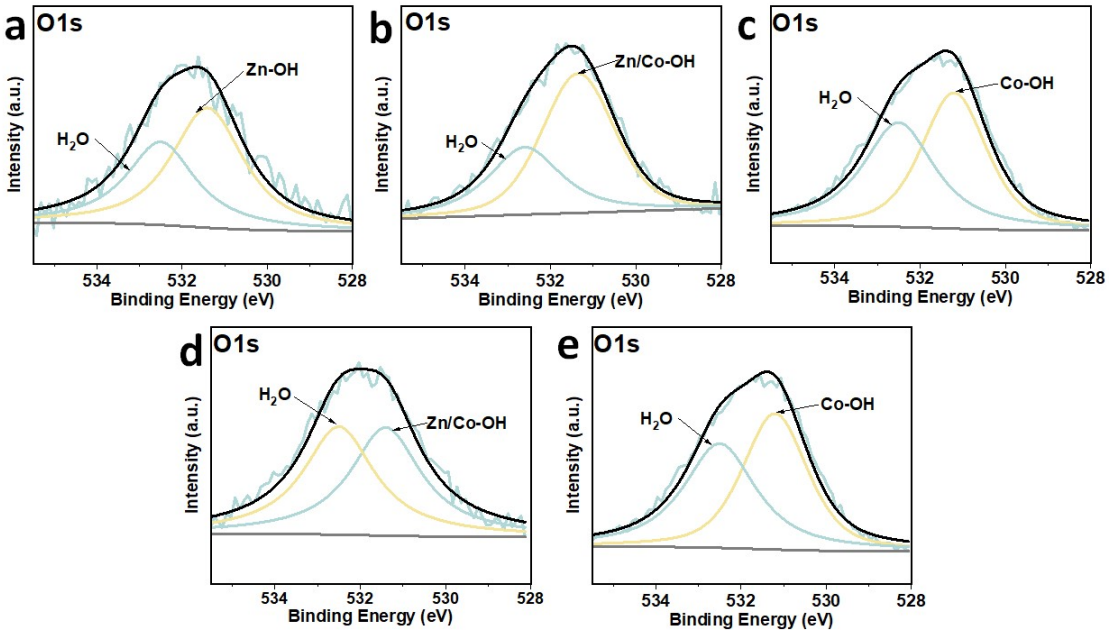

Fig. S15 O1s spectra of (a) $Zn_{10}Co_0$-mZIF-240, (b) Zn_7Co_3-mZIF-240, (c) Zn_5Co_5-mZIF-240, (d) Zn_3Co_7-mZIF-240 and (e) Zn_0Co_{10}-mZIF-240.

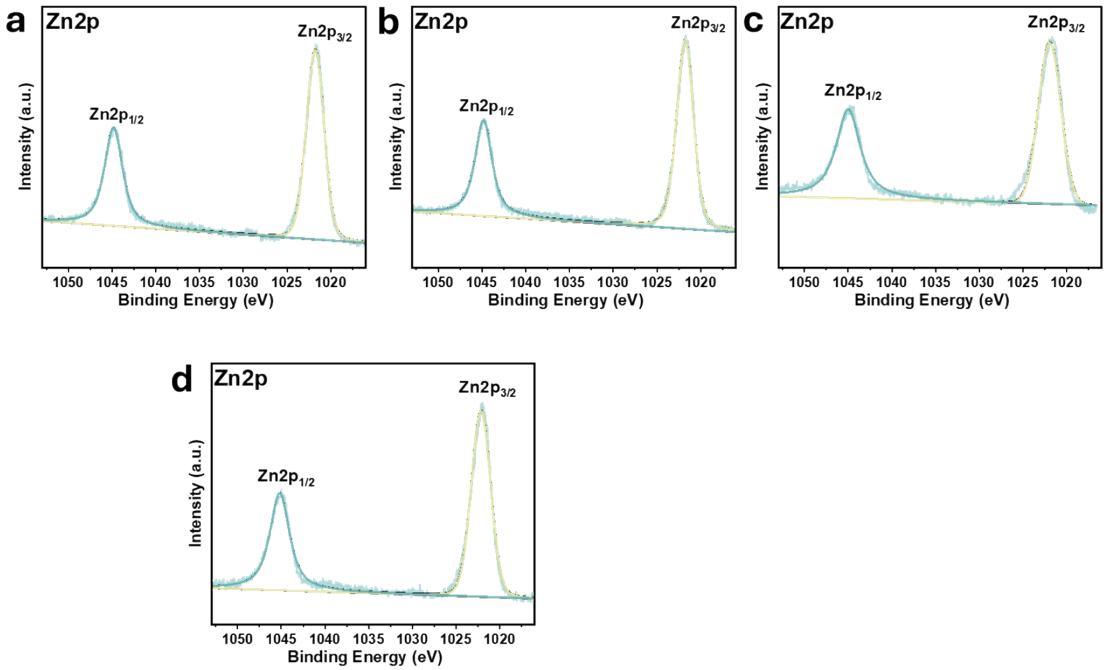

Fig. S16 Zn2p spectra of (a) $Zn_{10}Co_0$-mZIF-240, (b) Zn_7Co_3-mZIF-240, (c) Zn_5Co_5-mZIF-240 and (d) Zn_3Co_7-mZIF-240.

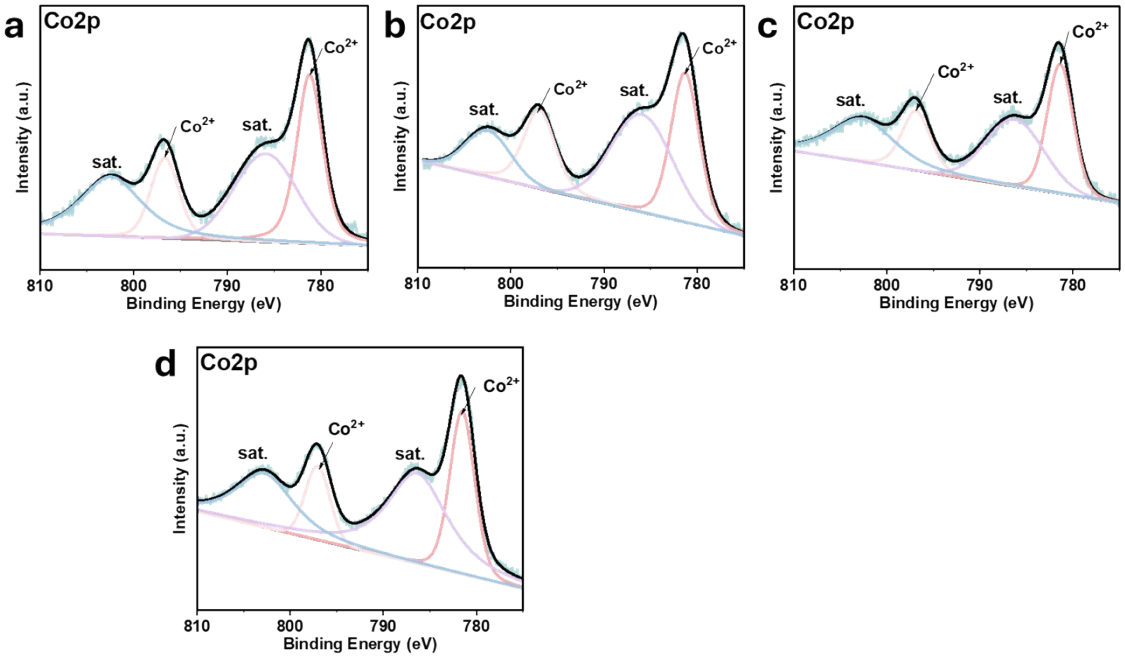

Fig. S17 Co2p spectra of (a) Zn_7Co_3-mZIF-240, (b) Zn_5Co_5-mZIF-240, (c) Zn_3Co_7-mZIF-240 and (d) Zn_0Co_{10}-mZIF-240.